Structures 36 (2022) 979–996

Contents lists available at ScienceDirect

Structures

journal homepage: www.elsevier.com/locate/structures

Improving ductility behavior of sway-special exterior beam-column joint using ultra-high performance fiber-reinforced concrete

Fayez R. Abusafaqa [a], Mohammed A. Samaaneh [a], Monther B.M. Dwaikat [b,*]

[a] Department of Civil Engineering, An-Najah National University, Nablus, Palestine
[b] Department of Building Engineering, An-Najah National University, Nablus, Palestine

ARTICLE INFO

Keywords:
Ultra-high performance concrete (UHPC)
Ductility
Reinforced concrete joints
Finite element modeling
ABAQUS
Nonlinear behavior

ABSTRACT

In the last decades, ductility of the joints becomes one of the most relevant issues in seismic design. Experiments show that the joints ductility is enhanced using additional transverse reinforcements. Thus, the design codes set requirements to attain the required level of ductility of joints including high amount of transverse reinforcement. However, the assemblage of many types of reinforcements causes implementations difficulties. This paper focuses on improving ductility of exterior beam-column joint (BCJ) using ultra-high performance concrete (UHPC) while dispensing the transverse reinforcements in the joint to overcome the implementations difficulties. A 3-D non-linear model using the finite element program ABAQUS is constructed and validated using published experimental data. After that, the model is used to conduct a parametric study that includes the main parameters affecting the behavior which include the beam to column depth ratio, the axial load ratio, and the longitudinal reinforcement ratio in column. The results of the parametric study are used to compare the behavior of sway-special joints and the joints strengthened with UHPC in terms of strength, ductility and the mode of failure. The results assure the ability of UHPC-strengthened joints to attain the required level of ductility and strength when compared to special moment resisting frame.

1. Introduction

1.1. Overview

In the last century, seismic codes requirements are not only based on the horizontal forces but also a reasonable level of ductility which enables the structure to sustain the seismic load [1]. However, the structural ductility, can be significantly reduced if brittle failure of joints occurs. Once brittle failure of joints occurs, a discontinuity of frame member is produced leading to structure failures at low levels of ductility as declared by Ghobarah and Said [2]. Thus, the ACI 352–02 committee [3] recommends that the joints should be upgraded by enhancing the effective core confinement or by increasing their shear capacity. In addition, current codes such as the ACI code [4] provide many design categories for designing joints under seismic loads. These categories which are classified based on sway level, region seismicity and construction importance; are ordinary, intermediate, and special sway. Each category presents a level of toughness. Clearly, as the level of ductility move from ordinary to special, the toughness (the energy that the system can dissipate), and the detailing requirements increase. However, the sway special category in design for seismic load is the most recommended. Although the sway special detailing shows some effectiveness, the assemblage of many types of reinforcements in the joints causes implementation difficulties [5]. Thus, many techniques were suggested to enhance the joints ductility such as the use of steel jacketing [6] and CFRP jacketing [7]. However, these techniques can be used in the post construction stage. Therefore, researchers developed many generations of cement based material reinforced with steel fibers that can enhance the ductility of concrete [8]. These generations include steel fiber reinforced concrete (SFRC), high strength fiber reinforced concrete (HSFRC) and ultra-high performance fiber reinforced concrete (UHPFRC).

1.2. Definition of UHPC

Extensive research has been conducted on studying the mechanical behavior of UHPC. This includes the work of Hakeem [9], Graybeal [10], Wuest et al. [1], Yoo & Yoon [11] and Prem et al. [12]. Although each researcher used different UHPC products with different mixing proportion and different behaviors, the UHPC share many characteristics such

* Corresponding author.
E-mail address: montherdw@najah.edu (M.B.M. Dwaikat).

https://doi.org/10.1016/j.istruc.2021.12.059
Received 16 February 2021; Received in revised form 27 September 2021; Accepted 20 December 2021
Available online 31 December 2021

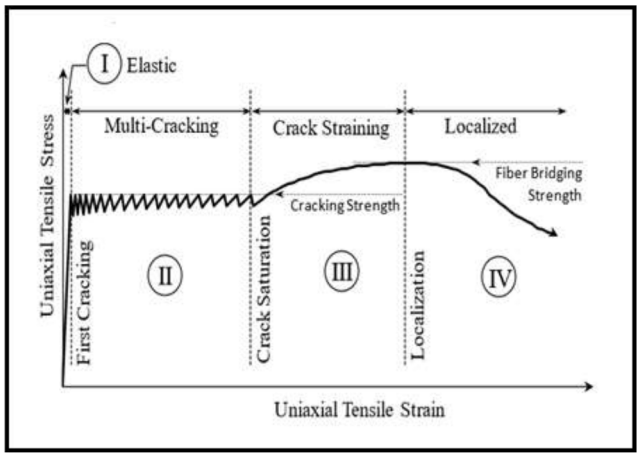

Fig. 1. Idealized tension behavior for UHPC. (FHWA [14].

as high compressive strength and low water cement ratio. In addition, this cement based material is often used with fibers; to enhance its tension behavior as indicated by Française de Génie [13]. The Federal Highway Administration (FHWA) [14] provides definition for the major properties of UHPC material and its mechanical behavior. It also approves six UHPC products, remarked as U-A through U-F, and studies there characteristics. The FHWA remarks that UHPC must have a multi crack zone allowing the material to go into stiffening and provide ductile tensile behavior. Fig. 1 shows the idealized tensile behavior as investigated by the FHWA [14].

2. Literature review

In the last decades, the techniques of using hybrid fiber reinforced materials attracted more attention for strengthening RC constructions. Many researchers investigated external strengthening techniques of beam column joints using different materials both numerically and experimentally [15–18]. Their studies focused on retrofitting systems using CFRP and shape memory alloy to improve capacity and ductility of exterior RC joints. On the other hand, a number of research studies investigated internal strengthening techniques. For example, Abu Tahnat and Halahla [19] studied the response of RC frames considering UHPC joints under seismic loading. They concluded that using such material transfers joints failure into beams and columns. In addition, Gencoglu and Eren [5] used SFRC to enhance the ductility of exterior

Table 1
Parameters for defining CDP model in ABAQUS.

Parameter symbol	Eccentricity ϵ	Dilation angle φ	biaxial stresses to the uniaxial stresses σ_{b0}/σ_{c0}	K_c
NC	0.1	36°	1.16	0.67
UHPC	0.1	36°	1.16	0.67

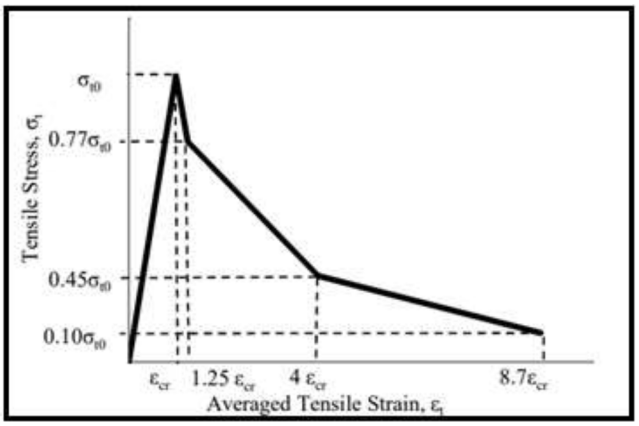

Fig. 3. Modified Nayal and Rasheed Model for ABAQUS. [36].

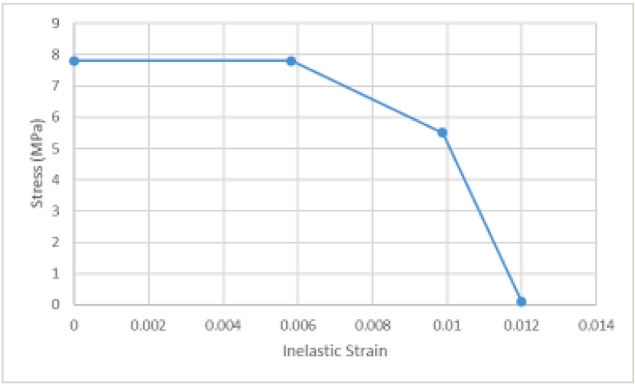

Fig. 4. Idealized stress-inelastic strain curve of UHPC class B.

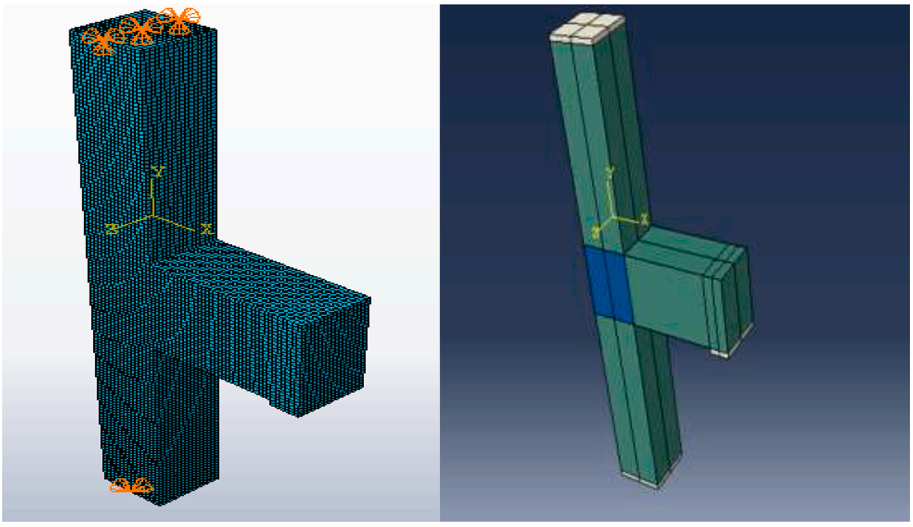

Fig. 2. The boundary conditions and the loading plates using in the model.

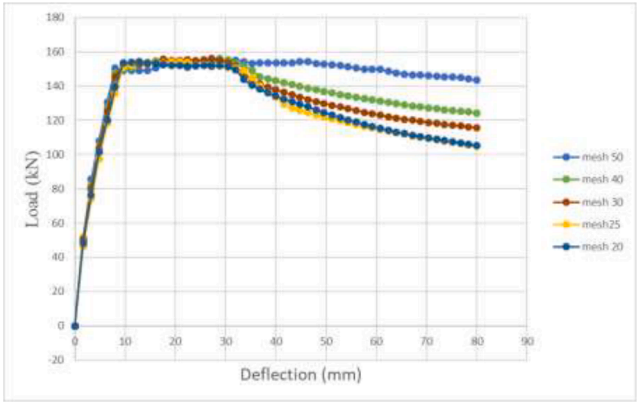

Fig. 5. Effect of mesh size.

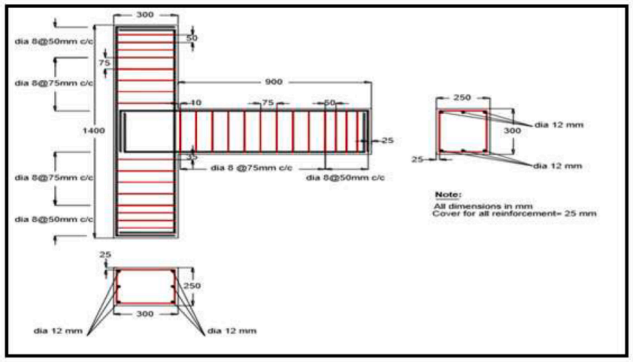

Fig. 6. Reinforcement Detailing and Dimensions for BCJ-12MM [8]

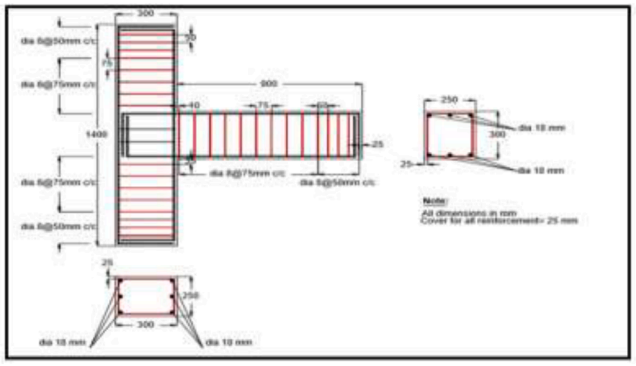

Fig. 7. Reinforcement Detailing and Dimensions for BCJ-S-18MM [8]

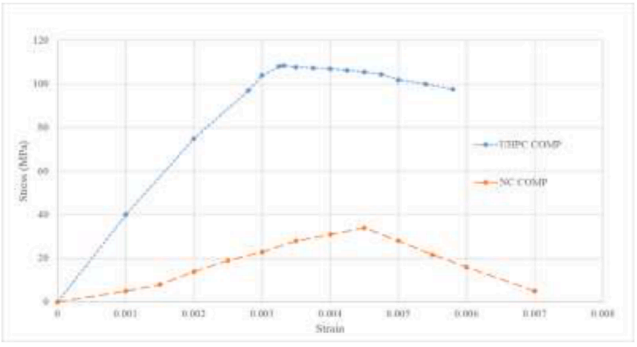

Fig. 8. Experimental Compressive Stress-Strain Curve for Normal Concrete and UHPC [8].

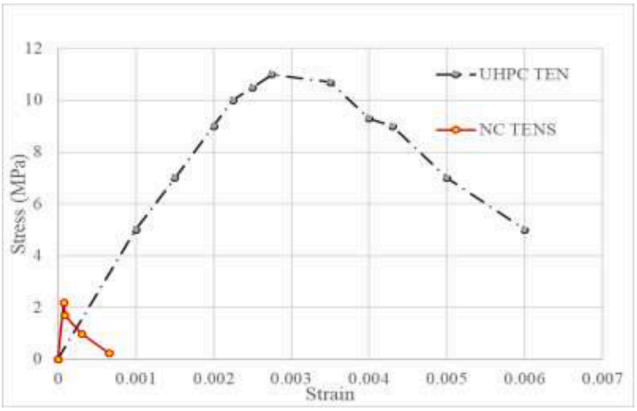

Fig. 9. Tensile Stress-Strain Behavior for UHPC and Normal Concrete [8].

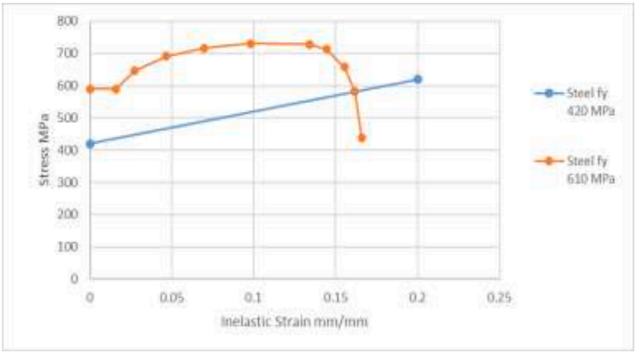

Fig. 10. Tensile Stress-Plastic Strain Curves Used in ABAQUS Modeling [8].

beam column joints. The results showed that the required amount of stirrups in the joints can be reduced using such material. Also, Shannag et al. [20] experimentally investigated the behaviors of high performance steel fiber reinforced concrete (HPFRC) beam-column joints. The results showed that the load carrying capacity, the energy dissipation and the stiffness degradation rate were enhanced by using HPFRC. Experimental investigation of the behavior of beam-column joints under cyclic loading was conducted by Ganesan et al. [21]. High strength concrete (HSC) of M60 grade with crimped steel fibers and polypropylene fibers was used in their specimens. Their results showed the possibility of reducing congestion of transverse reinforcement in beam-column joints through using HSC with fibers.

Further research considering internal strengthening of beam column joints was carried out by Alkhatib [8]. His research made comparisons between the behavior of exterior BCJs with different fiber reinforced materials and reinforcement detailing in the joint. Joints without transverse reinforcements faced flexural failure when using UHPC and SFRC. However, the study is limited to a column to beam moment capacity (CBM) ratio of more than two. Alkhatib [8] simulated the experimental test of the UHPC strengthened joints using ABAQUS software. The results showed that the concrete damage plasticity (CDP) with ABAQUS default values matched well with the experimental data. Chao et al. [22] tested two frames to investigate the effect of using the UHPC in plastic hinge zone without stirrups. One of the frames was a control specimen while the UHPC is used in the plastic hinge zone of the second frame. The two frames were tested under cyclic loading. The key finding of their research was that a minor damage occurred in columns when using UHPC. In addition, UHPC frames show higher strength and greater drift capacity.

Table 2
Parameters Used to Define CDP Model for Material Used by Alkhatib [8].

Material	Modulus of Elasticity E (MPa)	Poisson's Ratio	Dilation Angle ψ	K_c	σ_{b0}/σ_{c0}
NC Concrete	29,000	0.2	360	0.67	1.16
UHPC	40,000	0.2	360	0.67	1.16

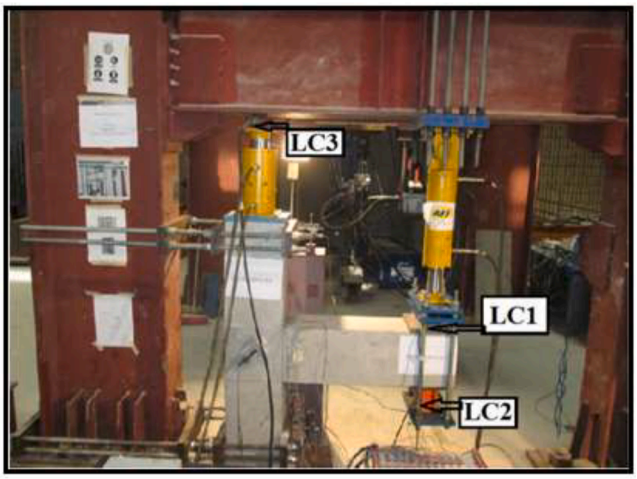

Fig. 11. Machine Test and Testing Conditions [8].

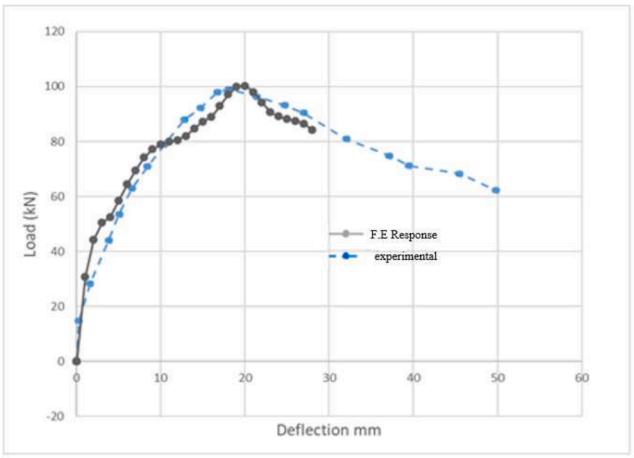

Fig. 13. Comparison between F.E and Experimental Results for Specimens NC-18MM tested by Alkhatib [8].

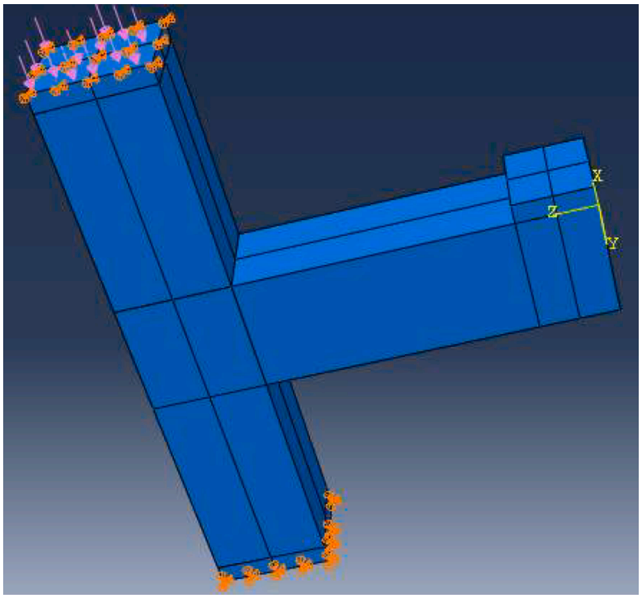

Fig. 12. ABAQUS Simulation for Specimens UHPC1-18MM and NC-18MM [8].

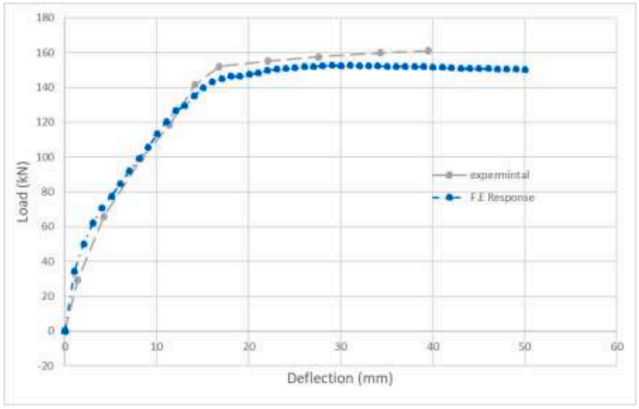

Fig. 14. Comparison between F.E and Experimental Results for Specimen UHPC-18MM Tested by Anas Alkhatib [8].

On the other hand, other researchers studied the use of external techniques of strengthening using fabric materials [23–25]. For example, Khan et al. [23] experimentally investigated the performance of exterior beam column joints strengthened with thin UHPC plates. They studied the joint behavior when attaching the UHPC plates to the substrate surface. The results showed the effectiveness of using UHPC jackets with sandblasting techniques in transferring the failure from shear failure at joint to preferable vertical flexure failure in the beam. The results also show the advantages of using cast-in-situ UHPC jacketing in terms of strength, stiffness and energy dissipation. Besides the experimental work, Khan et al. simulated the behavior of the exterior beam-column joints jacketed by 30 mm UHPC plates using ABAQUS software. The CDP model was used to model concrete. The study showed that CDP can be used to predict the behavior of such joints. Another research conducted by Chen and Graybeal [26] confirmed the reliability of CDP model in tracing the observed structural response. Chen and Graybeal modeled the structural behavior of the second generations of pi-girders strengthened by UHPC.

In addition, Al-Osta et al. [24] experimentally and numerically investigated the behavior of reinforced concrete beam strengthened with UHPFRC. Three strengthening configurations were used which are the bottom side strengthening, two-longitudinal-side strengthening and three-side strengthening. Two attachment techniques were used, namely: sand blasting technique and bonding using epoxy material technique. Experimental and numerical results showed a positive relation between the thickness of panel and the ductility of the strengthened beam in addition to the enhancement of the load carrying capacity. Beams strengthened at three sides had additional ductility and capacity improvements. However, the ductility of the beam strengthened on the bottom side was decreased. Also, Safdar et al. [25] experimentally investigated the behavior of reinforced concrete beam retrofitted with

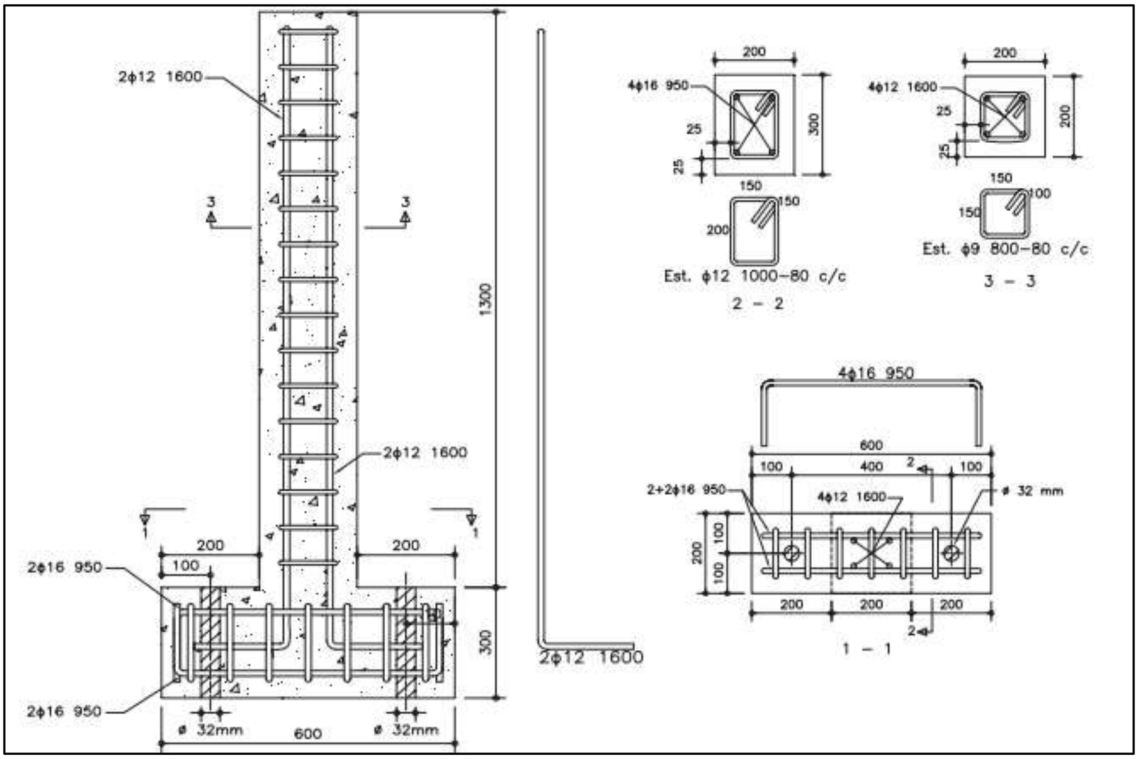

Fig. 15. Reinforcement and Dimensions of Selected Specimens [27]

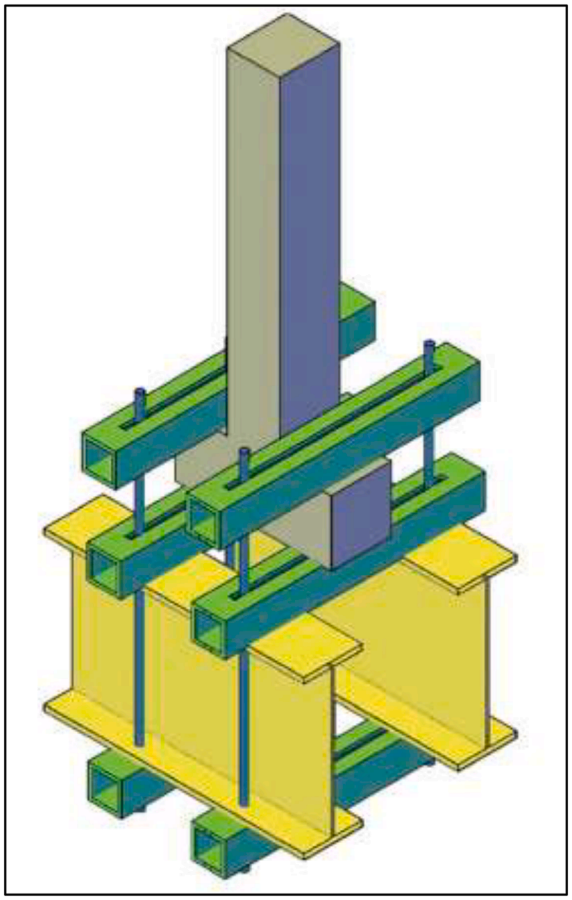

Fig. 16. Test Configuration for Sarmiento et al. Experiments [27]

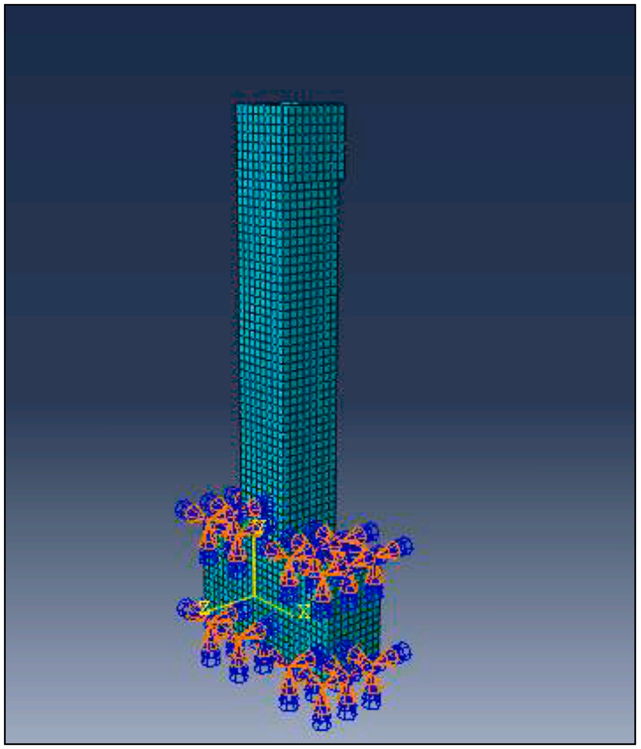

Fig. 17. ABAQUS Simulation for Specimens NC and UHPFRC-2% [27].

UHPFRC in the tension and compression zones. The results show that the flexure strength of the retrofitted beams was enhanced. More recently, Sarmiento et al. [27] tested seven specimens to investigate the effect of using UHPFRC on the behavior of interior BCJs. The joints were tested under cyclic loading and evaluated considering load–deflection

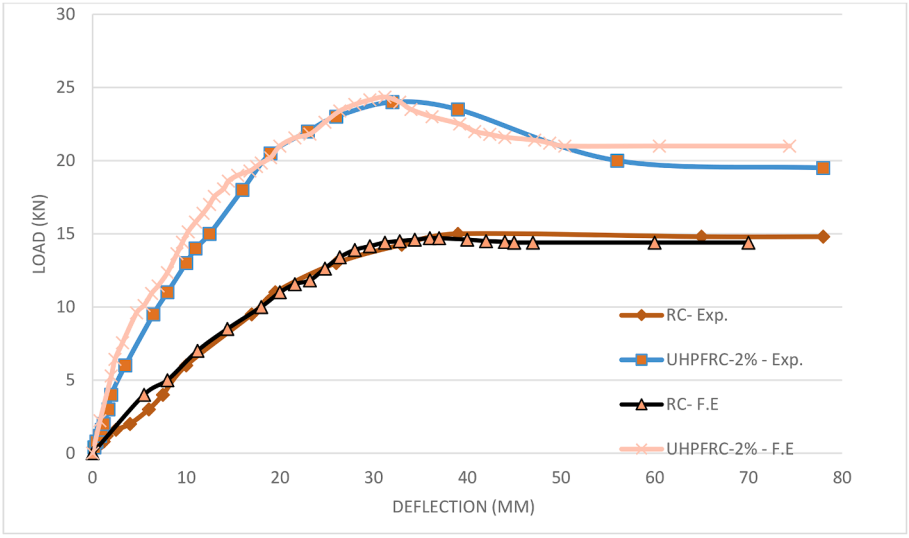

Fig. 18. Experimental vs. Numerical Load Deflection Curves of NC and UHPFRC-2% Specimens.

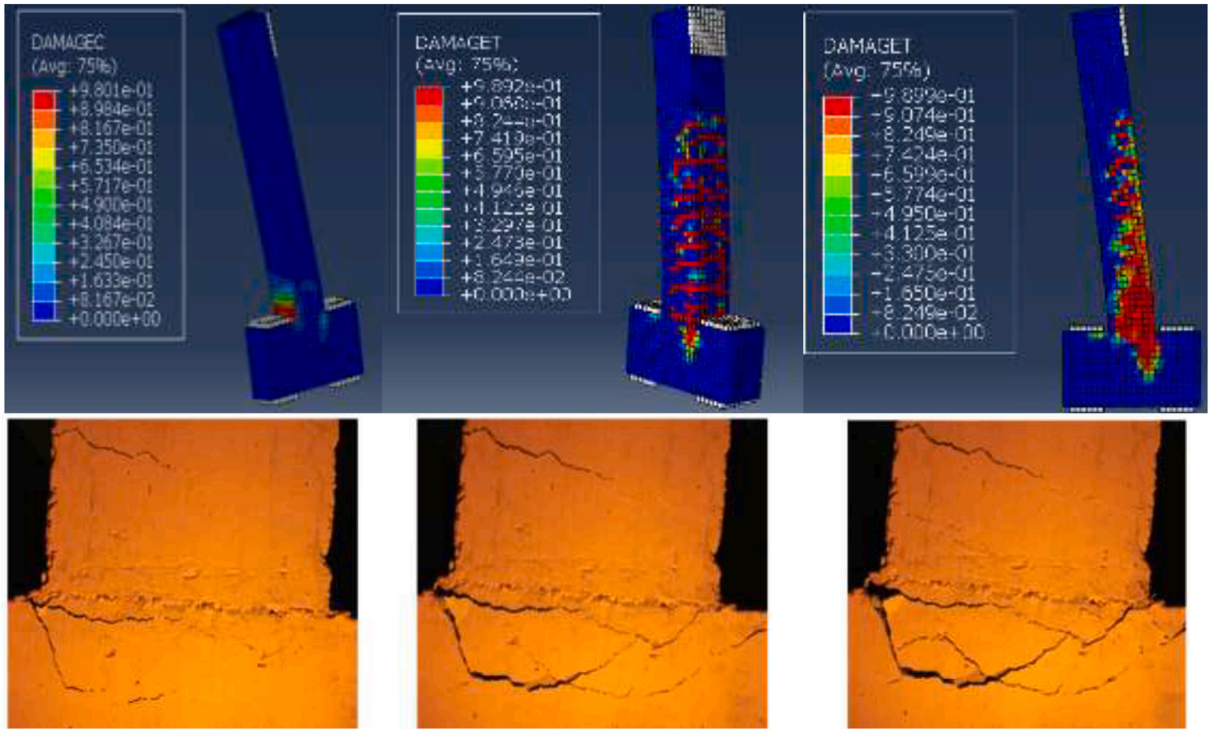

Fig. 19. Experimental vs. Numerical Crack Patterns of NC Specimen.

behavior, hysterical performance, stiffness degradation, and developed cracking pattern. They concluded that using UHPFRC increased the energy dissipation and reduced stiffness degradation of the joint.

The use of UHPC is extended for other structural applications such as Hung et al. [28]. Eight UHPC slender columns under eccentric load with different volumetric fracture of fiber were tested by Hung et al. The key parameters of the study were the volumetric fracture of fiber and the amount of transverse reinforcements. The results show that inclusion of steel fiber with volumetric fracture of 0.75% effectively restrained spalling and crushing of the slender UHPC column. In addition, using 1.5% volumetric fracture of fiber can compensate 70% reduction in the confinement steel with no reduction in ductility. Another research was performed by Racky [29] on comparisons between NC, HSC and UHPC. The materials were examined regarding to their cost-effectiveness and sustainability. The study was conducted using designed columns. The columns have the same load carrying capacity and ductility. The results showed that the use of UHPC produces lower life cycle costs and provides higher floor surface area.

Based on the literature survey, limited studies are conducted on the ductility of the joints internally strengthened with UHPC and hence the behavior of such joints is still not fully understood. Therefore, this research focuses on the ductility behavior of exterior BCJs strengthened with UHPC in comparison to that of sway-special exterior joints. UHPC class B as recognized by FHWA [14] with 2% volumetric fracture of fibers is considered in this research to improve the ductility behavior of the sway-special exterior BCJs. A numerical model will be developed for the exterior BCJ using ABAQUS software. The CDP model with it's default values in ABAQUS is used since it proved to produce reliable

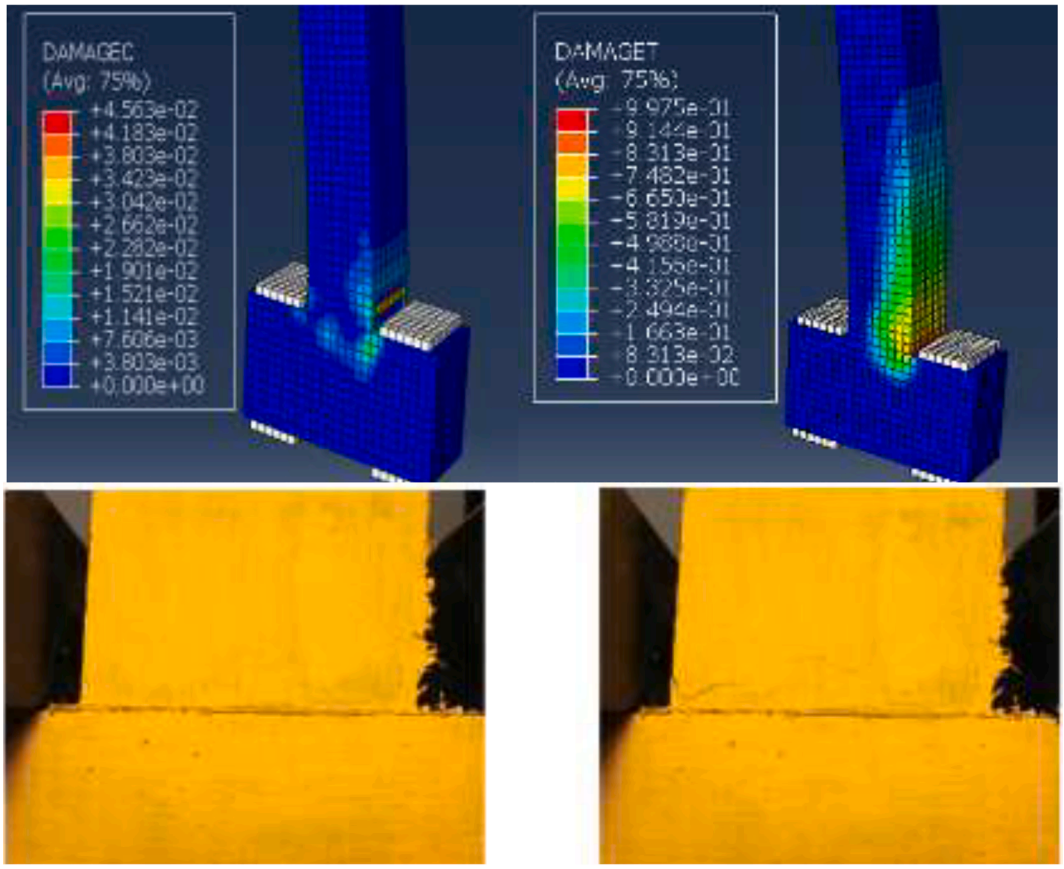

Fig. 20. Experimental vs. Numerical Crack Patterns of UHPFRC-2% Specimen.

Table 3
Constant Dimensions in the System.

Dimension	Value (m)
Floor Clear Elevation.	3.4
Width of the Column	0.5
Depth of the Column	0.5
Width of the Beam	0.5

results as confirmed by many researchers [8,23,26].

3. Numerical Modeling.

A computer model is constructed using the computer program ABAQUS [30] to investigate the behavior of exterior BCJ strengthened with UHPC and the possibility of improving the joint ductility. It is worth mentioning that ABAQUS, as a finite element tool, has been widely used for investigating the nonlinear behavior of RC structural members considering different material models such as CDP, and Smeared Cracking Model [31–34]. ABAQUS implicit dynamic approach is used in the analysis.

3.1. Modeling procedure

The model geometry is developed using a set of parts including beam, columns, joint and loading plates, in addition to reinforcements. The beam, column, joint and loading plate are modeled using an eight-node linear brick element (C3D8R), while the reinforcement (longitudinal, transverse) is modeled using a 2-node linear 3-D truss element (T3D2).

Three loading plates are applied to avoid the excessive stresses in the two columns ends and the tip of the beam for monotonic loading, while additional loading plate in the opposite tip of beam is used for cyclic loading. Half of the columns are modeled. Hence, the boundary conditions at the mid-section are assumed pins. Thus, the bottom surface was pinned at the line nodes at the center, while the top surface where released to move at Y-direction. The axial load is applied to the top surface of the column as a uniform pressure. A perfect bond is assumed between reinforcement bars and concrete. Fig. 2 shows the boundary condition and the loadings plates used in modeling.

3.2. Materials properties

The concrete damage plasticity (CDP) model in ABAQUS is used to capture the behavior of concrete and UHPC due to its capability of capturing the behavior under cyclic and monotonic loading. A set of input parameters are needed in addition to the stress-inelastic strain curve and the damage-inelastic strain curve. Table 1 summarizes the parameters used in defining CDP with defaults values assumed by ABAQUS. The models constructed based on these values showed good match with the experimental data as discussed in the literature review and reported by a number of researchers [8,23,26].

The stress–strain model proposed by Saenz [35] is used to describe the uniaxial compression behavior for the ordinary concrete in compression. The tension stress-inelastic strain curve is constructed using the modified Nayal and Rasheed [36] model, which is given in equations (1–7) and shown in Fig. 3.

$$\sigma_c = \frac{E_c \varepsilon_c}{1 + (R + R_E - 2)\frac{\varepsilon_c}{\varepsilon_0} - (2R - 1)\left(\frac{\varepsilon_c}{\varepsilon_0}\right)^2 + R\left(\frac{\varepsilon_c}{\varepsilon_0}\right)^3} \quad (1)$$

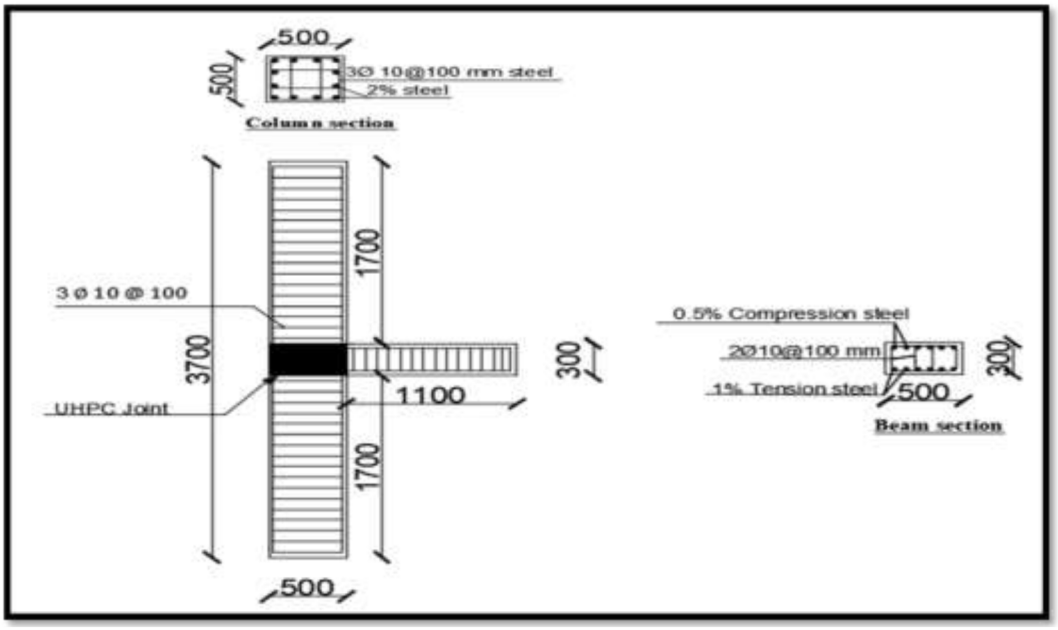

Fig. 21. Detailing of the simulation UB2-BCDR 0.6-L2.

Table 4
The Value of the Key Factors Affecting the Joints Behavior in the Study.

Parameter	Syllables
Joint Type	SP: for sway-special detailing jointUB2: for joint strengthened with UHPC class b with 2% volumetric fracture of fiber
Beam to column depth ratio	BCDR
Longitudinal reinforcement ratio in the column (ρ_c)	L1: for 1%L2: for 2%
Axial load ratio	ALR

$$E_c = 4700\sqrt{f_c^{'}} \tag{2}$$

$$R = \frac{R_E(R_\sigma - 1)}{(R_\varepsilon - 1)^2} - \frac{1}{R_E} \tag{3}$$

$$R_E = \frac{E_c}{E_0} \tag{4}$$

$$R\sigma = \frac{f_c^{'}}{\sigma_f} \tag{5}$$

$$R_\varepsilon = \frac{\varepsilon_f}{\varepsilon_0} \tag{6}$$

$$E_0 = \frac{f_c^{'}}{\varepsilon_0} \tag{7}$$

where σ_c, R, R_E, R_σ, R_ε, E_0, $f_c^{'}$, σ_f, ε_f and ε_0 are the compressive stress (MPa) corresponding to the compressive strain ε_c, relation ratio, modular ratio, stress ratio, strain ratio, secant modulus of elasticity, concrete compressive strength , stress at maximum strain (MPa), ultimate strain and the strain corresponding to the peak stress, respectively. R_σ and R_ε are considered to be 4.0 as reported by Hu and Evans [37].

For UHPC, the experimental tests conducted by FHWA [13] for the UHPC class B with 2% fiber content are used to describe the uniaxial compressive stress–strain behavior. While an idealized tensile behavior for the material is shown in Fig. 4.

The tension damage d_t and compression damage d_c are used to

Table 5
Variable Properties for all Models

Model ID	Joint Type	BCDR	ρ_c	ALR
SP-BCDR 0.6-L1-ALR 0.25	SP	0.6	1%	0.25
SP-BCDR 0.6-L1-ALR 05	SP	0.6	1%	0.5
SP-BCDR 0.6-L2-ALR 0.25	SP	0.6	2%	0.25
SP-BCDR 0.6-L2-ALR 0.5	SP	0.6	2%	0.5
UB2-BCDR 0.6-L1-ALR 0.25	UB2	0.6	1%	0.25
UB2-BCDR 0.6-L1-ALR 05	UB2	0.6	1%	0.5
UB2-BCDR 0.6-L2-ALR 0.25	UB2	0.6	2%	0.25
UB2-BCDR 0.6-L2-ALR 0.5	UB2	0.6	2%	0.5
SP-BCDR 1-L1-ALR 0.25	SP	1	1%	0.25
SP-BCDR 1-L1-ALR 05	SP	1	1%	0.5
SP-BCDR 1-L2-ALR 0.25	SP	1	2%	0.25
SP-BCDR 1-L2-ALR 0.5	SP	1	2%	0.5
UB2-BCDR 1-L1-ALR 0.25	UB2	1	1%	0.25
UB2-BCDR 1-L1-ALR 05	UB2	1	1%	0.5
UB2-BCDR 1-L2-ALR 0.25	UB2	1	2%	0.25
UB2-BCDR 1-L2-ALR 0.5	UB2	1	2%	0.5
SP-BCDR 1.2-L1-ALR 0.25	SP	1.2	1%	0.25
SP-BCDR 1.2-L1-ALR 05	SP	1.2	1%	0.5
SP-BCDR 1.2-L2-ALR 0.25	SP	1.2	2%	0.25
SP-BCDR 1.2-L2-ALR 0.5	SP	1.2	2%	0.5
UB2-BCDR 1.2-L1-ALR 0.25	UB2	1.2	1%	0.25
UB2-BCDR 1.2-L1-ALR 05	UB2	1.2	1%	0.5
UB2-BCDR 1.2-L2-ALR 0.25	UB2	1.2	2%	0.25
Model ID	Joint Type	BCDR	ρ_c	ALR
UB2-BCDR 1.2-L2-ALR 0.5	UB2	1.2	2%	0.5
SP-BCDR 1.4-L1-ALR 0.25	SP	1.4	1%	0.25
SP-BCDR 1.4-L1-ALR 05	SP	1.4	1%	0.5
SP-BCDR 1.4-L2-ALR 0.25	SP	1.4	2%	0.25
SP-BCDR 1.4-L2-ALR 0.5	SP	1.4	2%	0.5
UB2-BCDR 1.4-L1-ALR 0.25	UB2	1.4	1%	0.25
UB2-BCDR 1.4-L1-ALR 05	UB2	1.4	1%	0.5
UB2-BCDR 1.4-L2-ALR 0.25	UB2	1.4	2%	0.25
UB2-BCDR 1.4-L2-ALR 0.5	UB2	1.4	2%	0.5
SP-BCDR 1.6-L1-ALR 0.25	SP	1.6	1%	0.25
SP-BCDR 1.6-L1-ALR 05	SP	1.6	1%	0.5
SP-BCDR 1.6-L2-ALR 0.25	SP	1.6	2%	0.25
SP-BCDR 1.6-L2-ALR 0.5	SP	1.6	2%	0.5
UB2-BCDR 1.6-L1-ALR 0.25	UB2	1.6	1%	0.25
UB2-BCDR 1.6-L1-ALR 05	UB2	1.6	1%	0.5
UB2-BCDR 1.6-L2-ALR 0.25	UB2	1.6	2%	0.25
UB2-BCDR 1.6-L2-ALR 0.5	UB2	1.6	2%	0.5

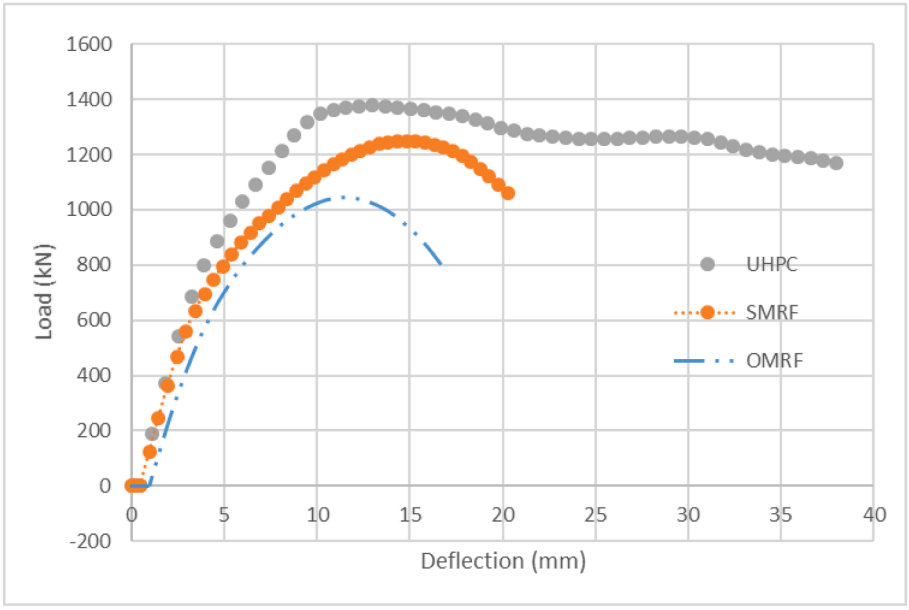

Fig. 22. Effect of the Detailing and the Material of the joint on the Behavior of the Simulation (BCDR1.6-L2-ALR0.25).

characterize the degradation in strength and stiffness in the softening behavior of the material. However, there are many models to evaluate the damage including Luccioni et al. [38] model, Burlion et al. [39] model, and Birtel and Mark [39]. In Birtel and Mark [40] model the damage in both tension and compression is related to the parameters b_c and b_t as given by Eqs (8) & (9), respectively. A value of 0.7 is often used for both parameters tension damage (Nasrin et al. [41], Al-Osta et al. [42] and Khan et al. [22]. This model is used to evaluate the damage parameters for concrete and UHPC.

$$d_t = 1 - \frac{\sigma_t E_c^{-1}}{\varepsilon_t^{pl}\left(\frac{1}{b_t} - 1\right) + \sigma_t E_c^{-1}} \tag{8}$$

$$d_C = 1 - \frac{\sigma_c E_c^{-1}}{\varepsilon_c^{pl}\left(\frac{1}{b_c} - 1\right) + \sigma_c E_c^{-1}} \tag{9}$$

Finally, an elastic-perfectly plastic model for steel grade 60 (420 MPa) is used for simplicity. The fracture strain of the steel was captured from local laps and it was taken as 0.18.

3.3. Model Validation.

Beam-column joint models are developed and verified using the experimental results of Alkhatib [8] and Sarmiento et al. [27]. Two representative specimens are selected from Alkhatib research to develop and validate the model, namely UHPC-18MM-BCJ and NC-18MM-BCJ. In addition, two specimens of Sarmiento et al. work are selected for further validation. Sensitivity study is conducted to obtain the suitable mesh size of the models. Fig. 5 shows the load deflection curves for UHPC-18MM-BCJ specimen in Alkhatib work with mesh size varying between 20 mm and 50 mm. It can be seen from Fig. 5 that mesh size of 25 mm produces reasonable accuracy, and hence this mesh size is used for all models in this paper.

3.3.1. Experiments by Alkhatib [8]

The specimens have identical reinforcement details and dimensions as illustrated in Fig. 6 **and** Fig. 7. The compressive behavior of NSC and UHPC used are shown in Fig. 8**,** while Fig. 9 shows the tensile stress–-strain behavior for UHPC and NC.

The stress-plastic strain curve for all bars is extracted from the reported data and used in ABAQUS model as shown in Fig. 10. All the steel bars have modulus of elasticity (E_s) 200 GPa and poisson's ratio (ν = 0.3). A bi-linear stress–strain model is used to describe the hardening behavior in the transverse reinforcements with slope hardening of 0.01 E_s as proposed by Ashour and Elmezaini [43].

Table 2 summarizes the main parameters used in defining the CDP model for both concrete and UHPC. These parameters include reported material properties; modulus of elasticity, poisson's ratio, and others captured from literature including: dilation angle ψ, K_c, f_{b0}/f_{c0} and the eccentricity [7,10,21–22].

The specimens were subjected to constant axial load of 150 (kN). After that, the response is traced under monotonic loading (displacement control). The boundary conditions are assumed to resist rotations based on the test conditions shown in Fig. 11. Fig. 12 shows the boundary conditions introduced at column ends.

Finally, a comparison between the F.E and experimental results for specimens NC-BCJ-18 mm and UHPC-BCJ-18MM are shown in Fig. 13 and Fig. 14, respectively.

The comparisons show that the model almost captured the overall behavior of the experiments. This model is used to investigate the main features that affect ductility behavior of BCJ.

3.3.2. Experiments by Sarmiento et al. [27]

Two specimens of Sarmiento et al. work are used for validation, one of which is made of normal concrete and named NC, while the other is made of with UHPFRC having 2% of fibers and named UHPFRC-2%. Fig. 15 shows the reinforcement and dimensions used in the two specimens while Fig. 16 shows the test configuration.

The compressive strength of concrete in the NC specimen is 21 MPa while it is 154 MPa for the UHPFRC-2% specimen. The stress–strain model proposed by Saenz [35] is considered in the analysis for the two specimens. Also, CDP model and its default values in ABAQUS (given in Table 2 are used in the analysis. Fig. 17 shows the constructed model with the required mesh and boundary conditions.

Results from the numerical models are compared to the experimental data as shown in Fig. 18. It can be seen that the models provide sufficient accuracy in predicting the experimental elastic and inelastic response. A comparison between the cracking patterns of tested specimens and the numerical results shows that the model is capable of capturing the cracking patterns with sufficient accuracy as shown in Figs. 19 and 20 for NC and UHPFRC-2% specimens, respectively.

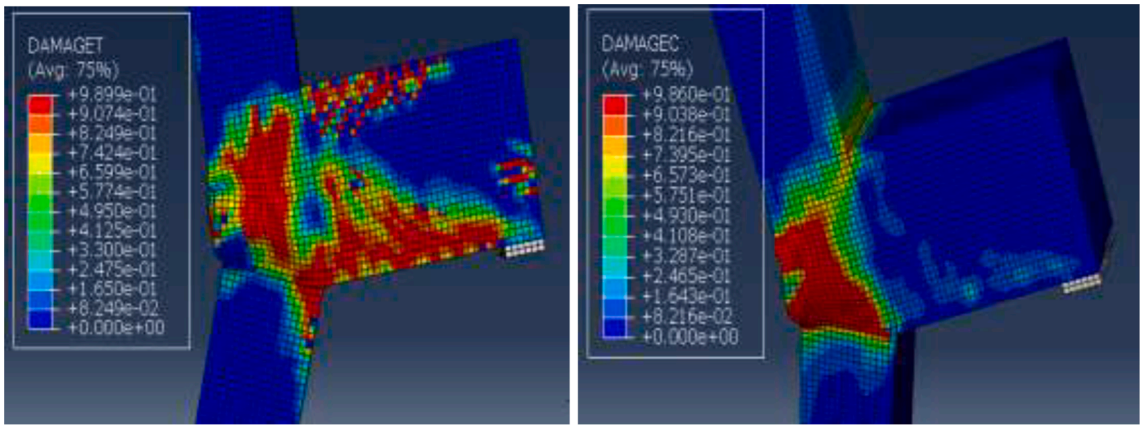

a) Tensile (Left) and Compressive (Right) Damages in OMRF Joint.

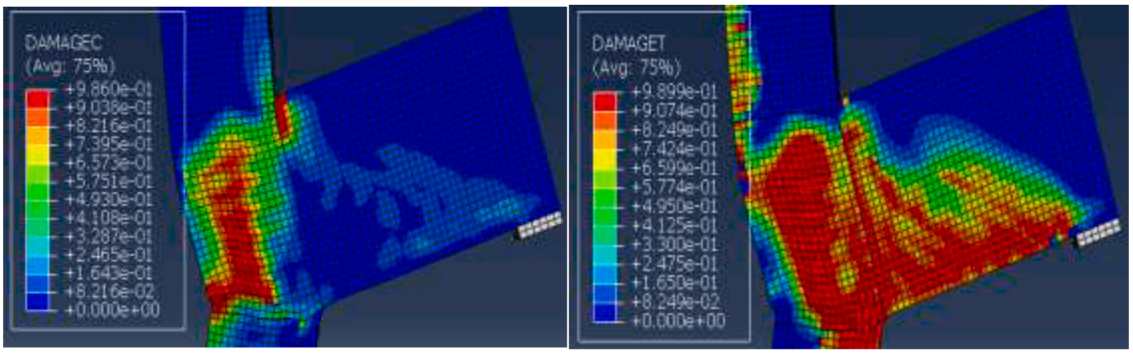

b) Tensile (Left) and Compressive (Right) Damages in SMRF Joint.

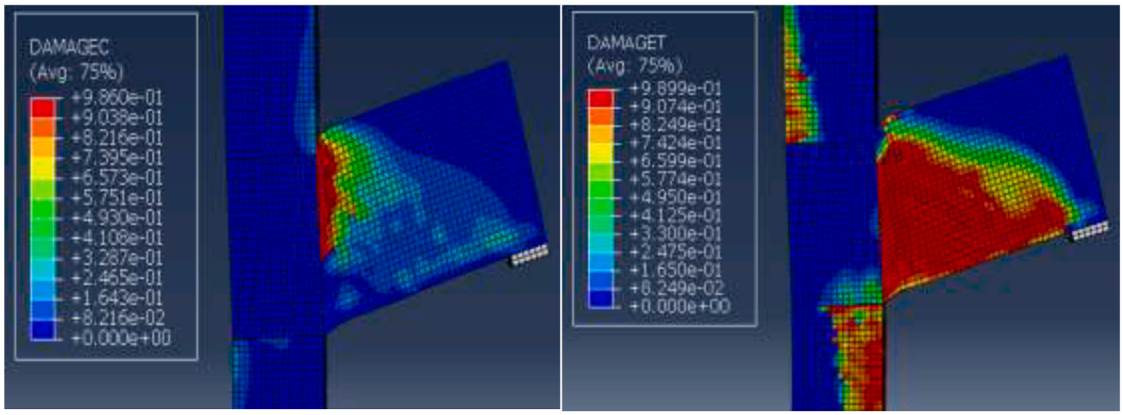

c) Tensile (Left) and Compressive (Right) Damages in UHPC Joint.

Fig. 23. Tensile and Compressive Damages in the Joints.

3.4. Parametric study

3.4.1. General

In order to study the behavior of the exterior beam column joints strengthened with UHPC. The key factors affecting the joints behaviors are divided into three branches which are factors affecting the shear capacity of the joints, factors affecting the development length of reinforcement bars and others affecting the column to beam moment capacity (CBM) ratio. However, the sway special design requires avoiding brittle failure modes using considerable amount of transverse reinforcement and providing sufficient development length. Thus, a factor characterizing the CBM ratio is considered. These factors are the beam to column depth ratio (BCDR), the longitudinal reinforcements in columns (ρ_c) and the axial load ratio (ALR) in columns. Table 3 presents the assumed dimensions in the BCJ.

The range of parameters considered and the parametric matrix conducted based on these parameters are given in the following section.

3.4.2. Range of parameters

In this research, a total of 40 simulations are carried out to investigate the ductility of using UHPC in BCJ and check the ability of UHPC to improve the ductility of exterior BCJs without using the sway special

Table 6
Effect of Varying ALR in the Ductility of SP Joints.

Parameter		SP		
BCDR	ALR	Ultimate Deflection	Yield Deflection	Ductility
ρ_c = 1%.				
0.6	0.25	56.9	5.8	9.8
	0.5	60.4	5.8	10.4
1	0.25	43.3	7.0	6.2
	0.5	52.7	7.1	7.4
1.2	0.25	48.7	7.6	6.4
	0.5	50.6	7.6	6.6
1.4	0.25	42.0	8.9	4.7
	0.5	28.3	9.5	3.0
1.6	0.25	25.5	13.2	JF
	0.5	24.6	15.4	1.6
ρ_c = 2%.				
0.6	0.25	56.0	5.6	10.0
	0.5	55.3	5.8	9.6
1	0.25	46.6	6.5	7.1
	0.5	46.7	6.5	7.1
1.2	0.25	43.6	7.4	5.9
	0.5	51.3	7.4	6.9
1.4	0.25	41.6	8.4	4.9
	0.5	37.4	8.3	4.5
1.6	0.25	20.3	17.5	1.2
	0.5	21.2	11.9	1.8

Table 7
Effect of Varying ALR in the Ductility of UHPC

Parameter		UB2		
BCDR	ALR	Ultimate Deflection	Yield Deflection	Ductility
ρ_c = 1%.				
0.6	0.25	60.5	5.8	10.3
	0.5	58.0	5.7	10.2
1	0.25	45.4	5.4	8.4
	0.5	40.8	5.4	7.5
1.2	0.25	40.6	6.1	6.7
	0.5	39.3	6.1	6.5
1.4	0.25	31.5	7.9	4.0
	0.5	29.9	8.0	3.8
1.6	0.25	30.7	11.0	2.8
	0.5	25.5	9.8	2.6
ρ_c = 2%.				
0.6	0.25	56.1	6.0	9.4
	0.5	57.0	6.1	9.3
1	0.25	37.1	5.8	6.4
	0.5	38.3	5.6	6.8
1.2	0.25	39.4	7.3	5.4
	0.5	39.5	7.3	5.4
1.4	0.25	40.5	6.7	6.0
	0.5	36.5	7.0	5.2
1.6	0.25	38.0	8.5	4.5
	0.5	37.7	8.4	4.5

transverse reinforcement detailing. Hence, the behavior of RC joint strengthened with UHPC class B with 2% volumetric fracture of fiber is compared with the behavior of the sway-special detailing joint. The compressive strength of concrete f_c is 28 MPa. The longitudinal reinforcement ratio in the beam is kept at 1% in tension and 0.5% in compression. Fig. 21 shows the detailing of simulation UB2-BCDR 0.6-L2.

As presented in the previous sections, three key parameters affecting the CBM ratio are considered. Each simulation is given a representative name consist of four syllable's. These syllables are shown in Table 4. These syllables present the type of the joint, the BCDR, (ρ_c) and ALR. For instant, the simulations (UB2-BCDR 1.6-L1-ALR 0.25) means that material UB2 is used in strengthening the joints with BCDR equals 1.6, ρ_c equals 1% and ALR equals 0.25. Another simulation is SP-BCDR 1.4-L1-ALR 0.50, this name means a control sway-special detailing joint with BCDR 1.4, ρ_c 1%, ALR 0.5. Finally, Table 5 shows the variable properties for all models conducted in this study.

4. Results and discussion

In this paper, ductility is defined as the ratio of the ultimate deflection to the deflection corresponding to yielding of steel reinforcement (Park and Paulay [44], Cohn and Bartlett [45] and Azizinamini et al. [46]. The ultimate deflection is defined as the deflection that corresponds to a 15% reduction of the peak load in the post peak value unless a rupture in the reinforcement bars occurs. The yield deflection is defined as the deflection at the onset of yielding of the tensile reinforcement in the beam. This ductility definition is used for all models regardless of the mode of failure.

4.1. Effect of the detailing and the material on the behavior of the joints

In this section, a comparison of the behavior of three BCJs is performed. The beams and the columns are identical in dimensions and reinforcement detailing. The reinforcement detailing in the first joint is designed according to the ordinary moment resisting frame (OMRF), while it is designed according to the special moment resisting frame (SMRF) requirements in the second specimen. In the third specimen, UHPC is used in the joint. The behavior of these specimens is shown in Fig. 22.

As can be seen in Fig. 22, the specimen with UHPC shows effectiveness in strengthening the joint more than the SMRF specimen. The figure also shows that joint with UHPC attain higher ductility compared to SMRF joint and OMRF joint. The tensile and the compressive damages at failure for the three specimens are shown in Fig. 23.

4.2. Effect of Varying ALR on the behavior of the Joints.

Generally, increasing the ALR decreases the ductility of the reinforced concrete joint and enhances its behavior through minimizing the crack openings as investigated by Al-Osta et al. [42]. Beyond a certain

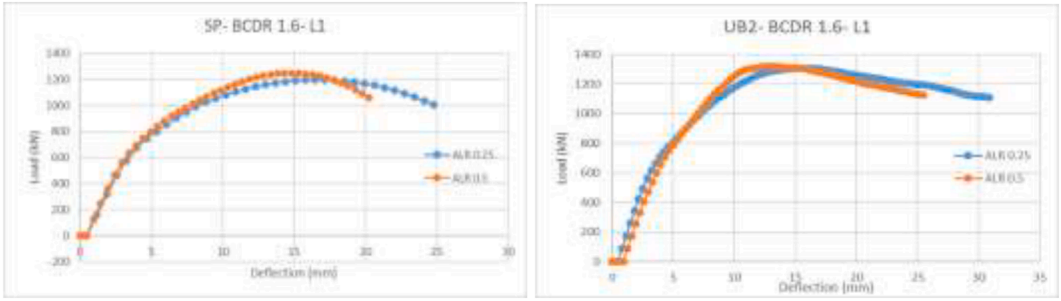

Fig. 24. Effect of ALR on the Behavior of Simulations BCDR1.6-L1. SP (left) and UB (right).

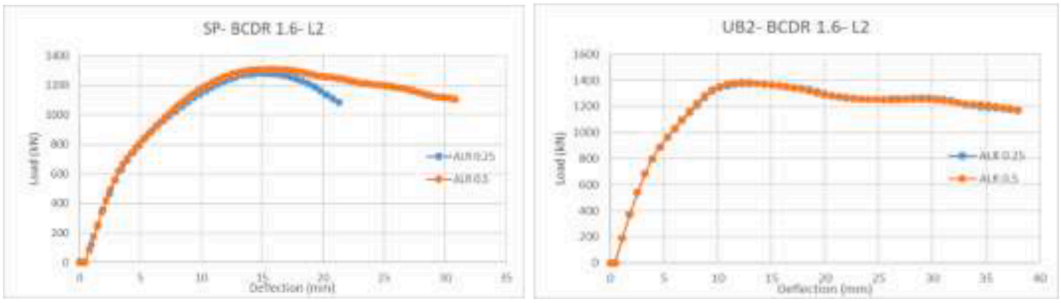

Fig. 25. Effect of ALR on the Behavior of Simulations BCDR1.6-L2. SP (left) and UB (right).

Table 8
Effect of Varying ρ_c in the Ductility of SP Joints with 0.25 ALR.

Parameter		SP		
BCDR	ρ_c	Ultimate Deflection	Yield Deflection	Ductility
ALR 0.25				
0.6	1%	56.9	5.8	9.8
	2%	56.0	5.6	10.0
1	1%	43.3	7.0	6.2
	2%	46.6	6.5	7.1
1.2	1%	48.7	7.6	6.4
	2%	43.6	7.4	5.9
1.4	1%	42.0	8.9	4.7
	2%	41.6	8.4	4.9
1.6	1%	25.5	13.2	1.9
	2%	20.3	17.5	1.2
ALR 0.5				
0.6	1%	60.4	5.8	10.4
	2%	55.3	5.8	9.6
1	1%	52.7	7.1	7.4
	2%	46.7	5.9	7.9
1.2	1%	50.6	7.6	6.6
	2%	51.3	7.4	6.9
1.4	1%	28.3	9.5	3.0
	2%	37.4	8.3	4.5
1.6	1%	24.6	15.4	1.6
	2%	21.2	11.9	1.8

Table 9
Effect of Varying ρ_c in the Ductility of UHPC Joints with 0.25 ALR.

Parameter		UB2		
BCDR	ρ_c	Ultimate Deflection	Yield Deflection	Ductility
ALR 0.25				
0.6	1%	60.5	5.8	10.3
	2%	56.1	6.0	9.3
1	1%	45.4	5.4	8.4
	2%	37.1	5.8	6.4
1.2	1%	40.6	6.1	6.7
	2%	39.4	7.3	5.4
1.4	1%	31.5	7.9	4.0
	2%	40.5	6.7	6.0
1.6	1%	30.7	11.0	2.8
	2%	38.0	8.5	4.5
Parameter		UB2		
BCDR	ρ_c	Ultimate Deflection	Yield Deflection	Ductility
ALR 0.5				
0.6	1%	58.0	5.7	10.2
	2%	57.0	6.8	8.4
1	1%	40.8	5.4	7.5
	2%	38.3	5.6	6.8
1.2	1%	39.3	6.1	6.5
	2%	39.5	6.0	6.6
1.4	1%	29.9	8.0	3.8
	2%	36.5	7.0	5.2
1.6	1%	25.5	9.8	2.6
	2%	37.7	8.4	4.5

Effect of Varying ρ_c in the Ductility of UHPC Joints with 0.25 ALR.

limit, the joint will suffer compression failure due to exceed the ultimate compressive capacity of the column. However, the behavior of sway-special detailing joint is different. While the increase in the ALR decreases the rotation of the joint due to reduction in cracking which reduces the deflection of the beam tip, the generated lateral strain due to the compressive stresses in the joint increases. Hence, the confinement effect increases. Consequently, the ductility can be positively affected. However, these two contradicting effects of the ALR, which are also affected by ρ_c and the depth of the neutral axis of the member, cause a fluctuation in the effect of the ALR on the ductility of the system. This fluctuation is reported by the experimental results of Bernardo and Lopes [47]. Table 6 shows the effect of ALR on the behavior of the sway-special joints.

The ALR decreases the rotation of the UHPC joint having no transverse reinforcement. Thus, the ductility decreases until a certain limit when the lower CBM ratio is violated. At that instance, the ALR plays a significant role in increasing the capacity of the confined core which in turn increases the capacity and the ductility of the system. Table 7 shows the effect of the same variable on UHPC joints.

It can be seen in Table 6 that the effect of ALR is more evident for high column to beam depth ratio (BCDR) of the SP joints while it is ignorant for low BCDR. On the other hand, Table 7 shows that small decrease in the ductility occurs with increasing the ALR for UHPC joints. Fig. 24 and Fig. 25 show the effect of ALR on the behavior of simulations BCDR1.6-L1 and BCDR1.6-L2, respectively. It can be seen from Tables 6 that the fluctuation in the ductility for SP joints is relatively high which consistent with the experimental results reported by Bernardo and Lopes [47]. This is related to the concrete cracking that is reflected by the location of neutral axis. However, this fluctuation is ignorant for UHPC joints as tabulated in Table 7. This can be mainly attributed to the ductile tensile behavior of UHPC that reduces cracking in the joint.

It can be seen from Fig. 24 and Fig. 25 that increasing the ALR slightly increases the load carrying capacity of the joint attributed to reduction in cracking in the joint.

For lower ρ_c the ultimate deflection decreases when increasing the ALR due to the decrease in the rotation of the joint, while for the higher ρ_c, increasing the ALR has ignorant effect on the behavior of UHPC. On the other hand, the ALR has positive effect on increasing the ductility of the SP joint at higher values of ρ_c. This is because increasing ρ_c contributes to shifting the failure from the joint to the beam of the model SP-

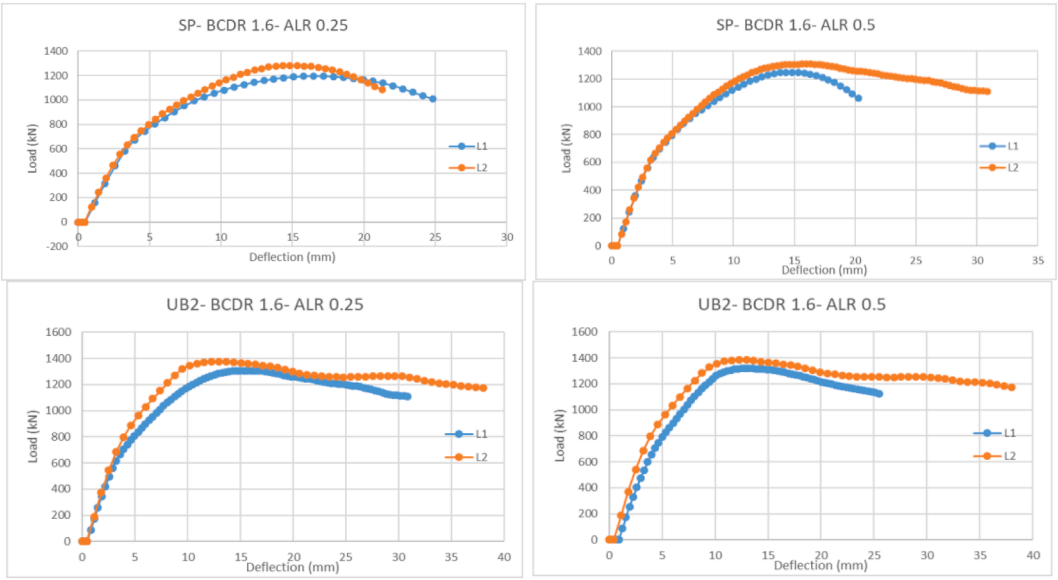

Fig. 26. Effect of Increasing ρ_c on the Behavior of SP joints (Top) and UHPC (bottom).

Table 10
Effect of Varying BCDR on the Ductility of SP Joints with ρ_c 1% and ALR 0.25.

Group	BCDR	Ultimate Deflection	Yield Deflection	Ductility
L1-ALR0.25	0.6	56.9	5.8	9.8
	1	43.3	7.0	6.2
	1.2	48.7	7.6	6.4
	1.4	42.0	8.9	4.7
	1.6	25.5	13.2	1.9
L1-ALR0.5	0.6	60.4	5.8	10.4
	1	52.7	7.1	7.4
	1.2	50.6	7.6	6.6
	1.4	28.3	9.5	3.0
	1.6	24.6	15.4	1.6
L2-ALR0.25	0.6	56.0	5.6	10.0
	1	46.6	6.5	7.1
	1.2	43.6	7.4	5.9
	1.4	41.6	8.4	4.9
	1.6	20.3	17.5	1.2
L2-ALR0.5	0.6	55.3	5.8	9.6
	1	46.7	5.9	7.9
	1.2	51.3	7.4	6.9
	1.4	37.4	8.3	4.5
	1.6	21.2	11.9	1.8

Table 11
Effect of Varying BCDR on the Ductility of SP Joints with ρ_c 1% and ALR 0.25.

Group	BCDR	Ultimate Deflection	Yield Deflection	Ductility
L1-ALR0.25	0.6	60.5	5.8	10.3
	1	45.4	5.4	8.4
	1.2	40.6	6.1	6.7
	1.4	31.5	7.9	4.0
	1.6	30.7	11.0	2.8
L1-ALR0.5	0.6	58.0	5.7	10.2
	1	40.8	5.4	7.5
	1.2	39.3	6.1	6.5
	1.4	29.9	8.0	3.8
	1.6	25.5	9.8	2.6
L2-ALR0.25	0.6	56.1	6.0	9.3
	1	37.1	5.8	6.4
	1.2	39.4	7.3	5.4
	1.4	40.5	6.7	6.0
	1.6	38.0	8.5	4.5
L2-ALR0.5	0.6	57.0	6.8	8.4
	1	38.3	5.6	6.8
	1.2	39.5	6.0	6.6
	1.4	36.5	7.0	5.2
	1.6	37.7	8.4	4.5

BCDR1.6. Hence, higher damage is transferred to the column. Thus, increasing the ALR increases the capacity of the column. Consequently, the capacity of the system increases and the confinement effect becomes more effective in increasing the ductility.

4.3. Effect of varying column longitudinal reinforcement ratio (ρ_c) on joints behaviors

In general, increasing the column longitudinal reinforcement increases the capacity and the stiffness of the column, causing a lower ultimate deflection in the joint. However, this increase in stiffness is opposed with a decrease in the axial stresses in the column and joint. Further, when severe damage in column occurs, the longitudinal reinforcement can control the overall behavior of the system and shift it from column failure to beam flexure failure in cases where joint failure is avoided. Tables 8 and 9 show the effect of ρ_c on the ductility of SP and UHPC joints, respectively.

Based on Tables 8 and 9, the ductility decreases with inceasing the longitudinal reinforcements in column up to BCDR = 1.4, while it increases for the models with BCDR = 1.6. Fig. 26 shows the effect of ρ_c on the behavior of SP and UHPC joints with BCDR 1.6.

It can be seen from Fig. 26 that the models with higher ρ_c have higher load carrying capacity, which reduces the damage and enhance the overall behavior of the system. However, the ultimate deflection is decreased for the simulation designated as SP-ALR0.25. This is mainly because the joint becomes more critical than the column at high deflection. In other words, increasing ρ_c has higher effect on the capacity of the column with small effect on the capacity of the joints.

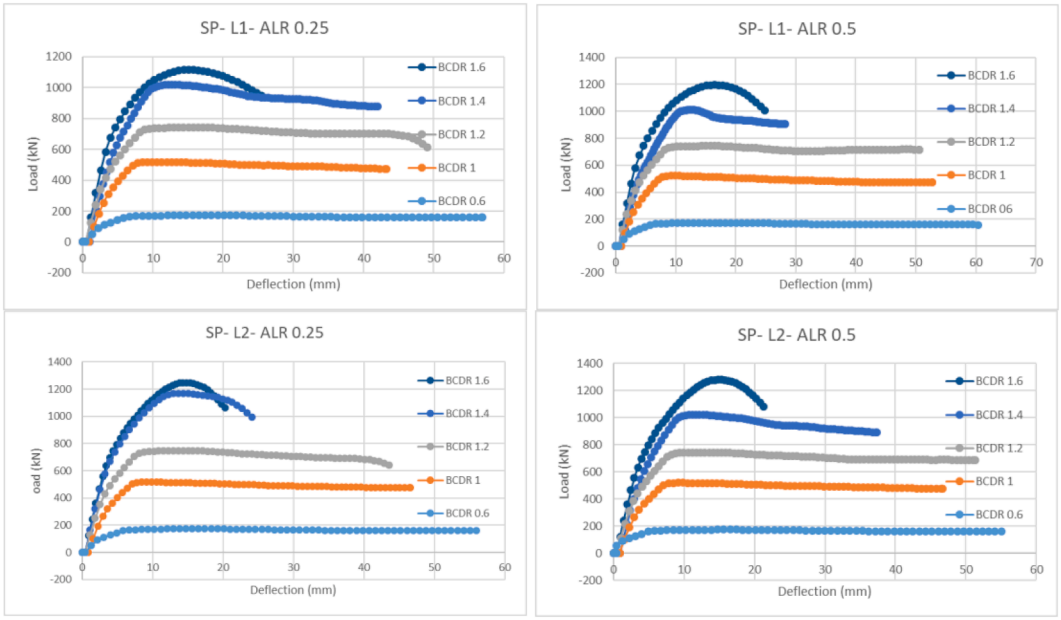

Fig. 27. Effect of Varying BCDR on the Behavior of SP Joints

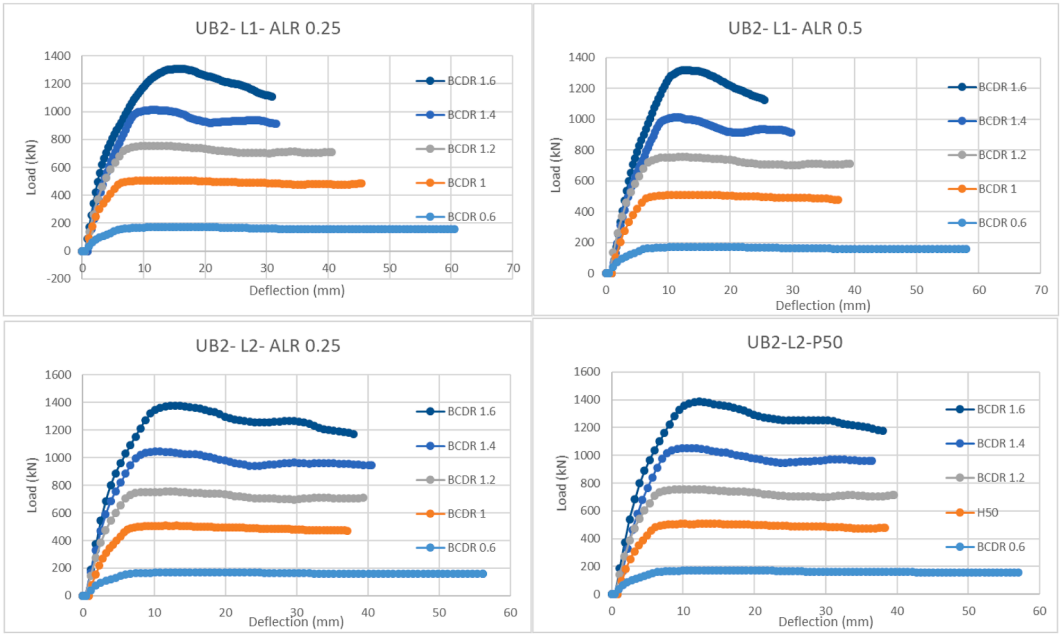

Fig. 28. Effect of Varying BCDR in the Behavior of UHPC Joints.

4.4. Effect of varying beam to column depth ratio (BCDR) on joints behaviors

In general, increasing the depth of the beam means increasing the moment capacity of the beam and transforming stresses to the joint and column, which causes more damage to the joint and reduces the ductility of the system. Table 10 and 11 show the effect of increasing the BCDR on the ductility of SP and UHPC joints, respectively.

It can be seen from Table 10 and 11 that the ductility decreases with increase the BCDR. However, the effect of BCDR is fluctuating as can be seen in Fig. 27 and Fig. 28.

It can be noticed from Fig. 27 and Fig. 28 that the ultimate deflection generally decreases with increasing the BCDR. However, the ultimate deflection for certain cases can be increased despite of the BCDR. This is mainly because the concrete in the column enters the inelastic range. Hence, a sudden drop in the stiffness occurs and causes this increase in the ultimate deflection.

For the simulations with BCDR 1.6, the BCM ratio exceeds the recommended value by the ACI 318–14 code. At this point, the cover spalls off and the capacity gradually decreased. Hence, the confinement effect

Table 12
Effect of Using UHPC on the Ductility of the Joints with 0.25 ALR.

ID	Parameters		SP			UHPC		
	BCDR	ρ_C	Ultimate Deflection	Yield Deflection	Ductility	Ultimate Deflection	Yield Deflection	Ductility
ALR0.25	0.6	1%	56.9	5.8	9.8	60.5	5.8	10.3
		2%	56.0	5.6	10.0	56.1	6.0	9.3
	1	1%	43.3	7.0	6.2	45.4	5.4	8.4
		2%	46.6	6.5	7.1	37.1	5.8	6.4
	1.2	1%	48.7	7.6	6.4	40.6	6.1	6.7
		2%	43.6	7.4	5.9	39.4	7.3	5.4
	1.4	1%	42.0	8.9	4.7	31.5	7.9	4.0
		2%	41.6	8.4	4.9	40.5	6.7	6.0
	1.6	1%	25.5	13.2	1.9	30.7	11.0	2.8
		2%	20.3	17.5	1.2	38.0	8.5	4.5
ALR0.5	0.6	1%	60.4	5.8	10.4	58.0	5.7	10.2
		2%	55.3	5.8	9.6	57.0	6.8	8.4
	1	1%	52.7	7.1	7.4	40.8	5.4	7.5
		2%	46.7	5.9	7.9	38.3	5.6	6.8
	1.2	1%	50.6	7.6	6.6	39.3	6.1	6.5
		2%	51.3	7.4	6.9	39.5	6.0	6.6
	1.4	1%	28.3	9.5	3.0	29.9	8.0	3.8
		2%	37.4	8.3	4.5	36.5	7.0	5.2
	1.6	1%	24.6	15.4	1.6	25.5	9.8	2.6
		2%	21.2	11.9	1.8	37.7	8.4	4.5

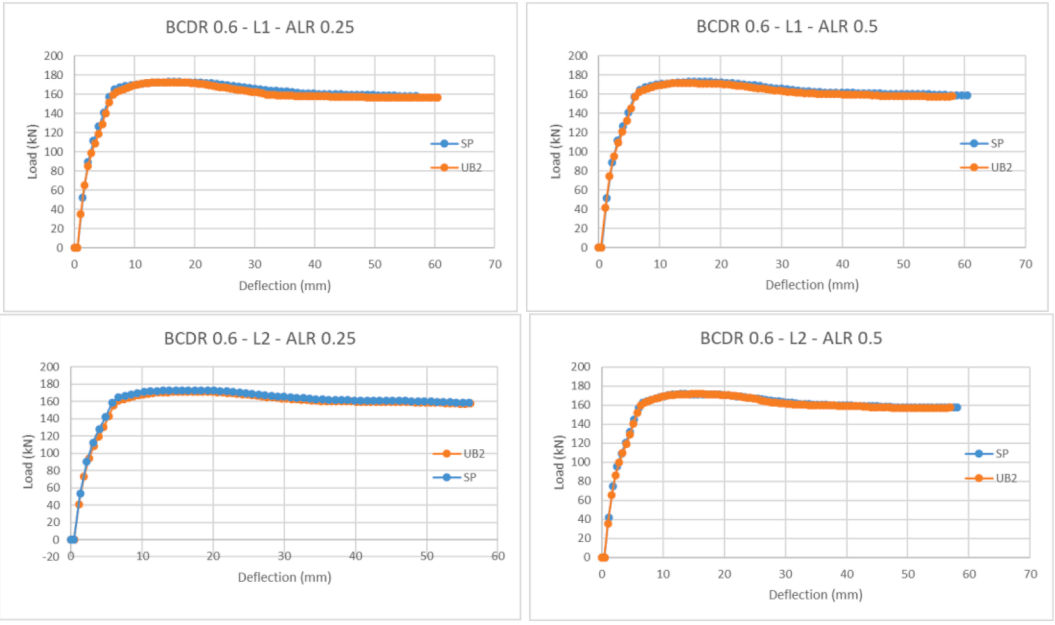

Fig. 29. Effect of Using UHPC in the Behavior of the Joints at BCDR 0.6.

on the core of the column plays a main role in securing the capacity of the column and avoiding sudden failure of the system. However, this decrease in the capacity contributes to the decrease in the ultimate deflection.

4.5. Effect of using UHPC on the behavior of the Joints.

In general, UHPC is very stiff and ductile compared to ordinary concrete. Thus, it shows effectiveness in strengthening the joints and save capacity until flexure ductile failure in beam occurs. Although UHPC joints show less deformation compared to sway-special joints, they show more ductility. This is because the yield deflection in UHPC joints is often less than that for the sway-special joints. In addition, the UHPC joints show less compression and tension damages at joint zone as shown in Fig. 23. These results emphasize the effectiveness of using UHPC instead of sway special detailing in concrete joints. Table 12 compares the results of SP and UHPC joints.

It can be seen in Table 12 that UHPC shows effectiveness in enhancing the joints ductility. However, using UHPC provides almost the same ductility as for sway special detailing when the value of BCDR is low, while it shows advantages compared to sway-special joints for high values of BCDR as can be seen in Fig. 29 and Fig. 30. Fig. 30 shows that UHPC joints show higher load carrying capacity compared to sway-special joints. In addition, the ductility is significantly increased. This

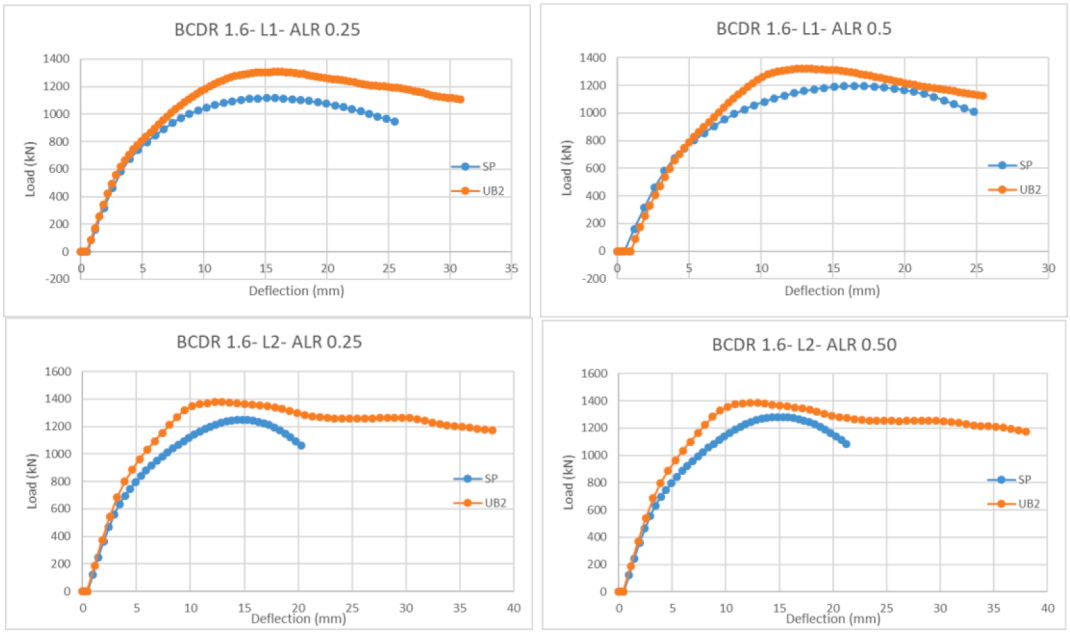

Fig. 30. Effect of Using UHPC in the Behavior of the Joints at BCDR 1.6.

Table 13
Cyclic load pattern.

Cyclic No	Drift Ratio	Push	Pull
	%	mm	Mm
1	0.5	5	−5
2	1.5	15	−15
3	3	30	−30
4	5	50	–

indicates the capability of UHPC in strengthening the joint and shifting the failure from the joint to the beam.

4.6. Comparison between UHPC and SP joints under cyclic Load.

Considering the fact that the sway-special detailing is used in design for seismic load, it is worth to compare the behavior of UHPC joints and sway-special joints under cyclic load. Hence, the model BCDR1.6-L2-ALR0.25 is used. Table 13 tabulates the cyclic load pattern applied to the tip of beam. Fig. 31 shows the load–deflection curves for SP and UHPC joints.

It can be seen from Fig. 31 that the UHPC joint show higher capacity compared to the SP joint. This is because UHPC joint has less damage and smaller cracks as can be seen in Fig. 32.

It is clear that UHPC shows more effectiveness in strengthening the joint comparing with sway-special detailing at the lower column to beam moment capacity ratio.

5. Conclusions

Based on the results of this research, the following conclusions can be drawn:

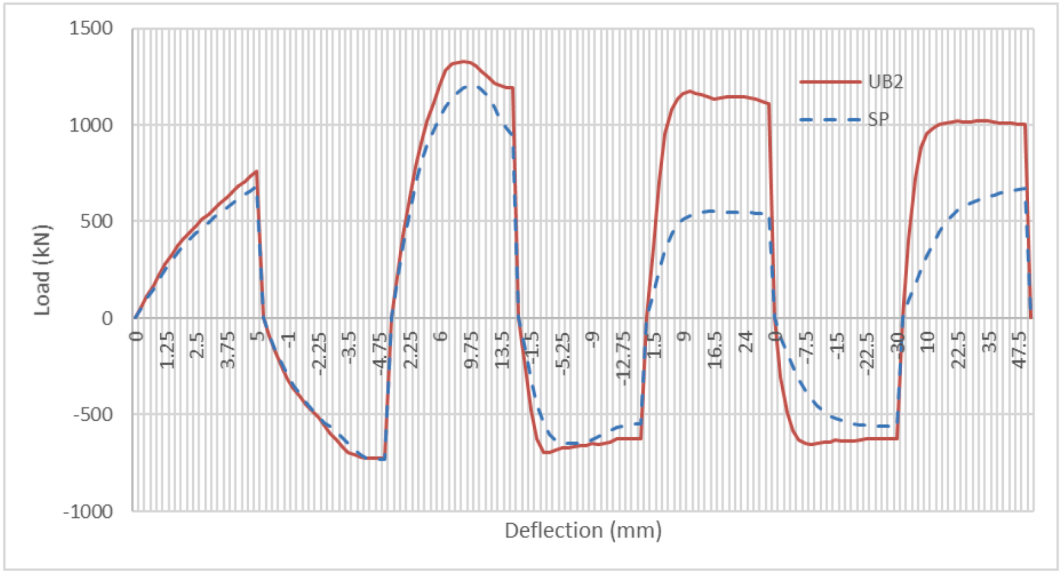

Fig. 31. Load-Deflection Curves for UHPC and SP Joint under Cyclic Load (BCDR1.6-L2-ALR0.25).

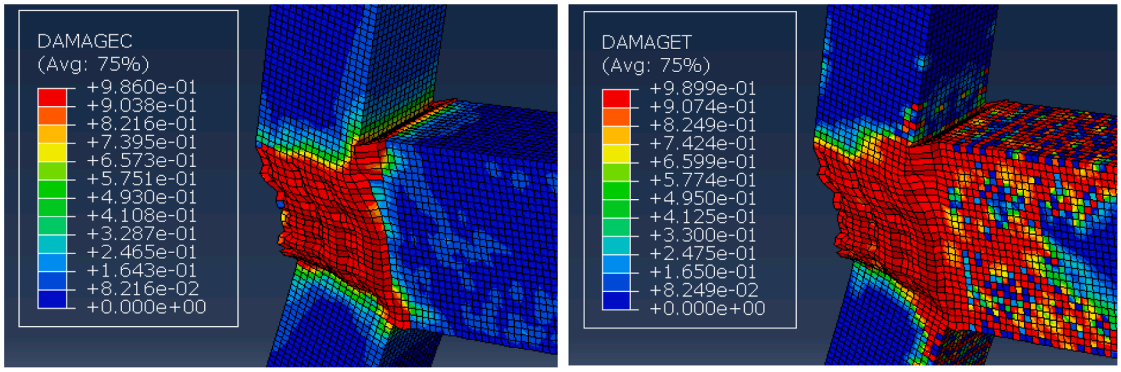

a) SP Joint.

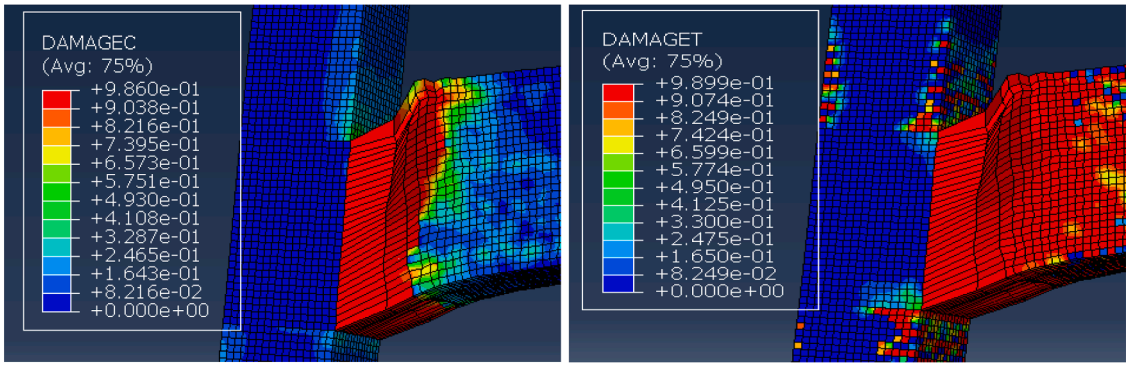

b) UHPC joint.

Fig. 32. Tensile and Compressive Damage in Simulation BCDR1.6-l2-ALR0.25 for: a) SP Joint and B) UHPC Joint.

- UHPC can be used to replace SP detailing in exterior beam column concrete joints without negative impact on joint ductility.
- The use of UHPC can significantly improve the ductility of exterior beam column concrete joints with high values of BCDR over those with SP detailing. Hence, using UHPC provide lower rehabilitation costs.
- The UHPC class B (with 2% volumetric fraction of fiber) shows effectiveness in strengthening the joints at high BCDR. Hence, UHPC classes with lower volumetric fractions of fiber may be used for low BCDR.
- The ALR have a negative effect on the ductility of exterior beam column joint till certain limit. Beyond this limit the ductility increases with increasing ALR.
- In general, increasing the longitudinal reinforcement of the column decrease the ductility of the joint. However, it can positively affect the ductility of the system for high values of BCDR.
- The UHPC shows effectiveness in securing the joints at BCM ratio violating the ones specified in the ACI 318 code while the sway-special detailing joints have high compressive damage.

Declaration of Competing Interest

The authors declare that they have no known competing financial interests or personal relationships that could have appeared to influence the work reported in this paper.

References

[1] Stanford University. Quake '06 Centennial Walking Tour. https://quake06.stanford.edu/centennial/tour/index.html, 2006.
[2] Ghobarah A, Said A. Shear strengthening of beam-column joints. Eng Struct 2002; 24(7):881–8.
[3] ACI-ASCE. Recommendations for Design of Beam-Column Joints in Monolithic Reinforced Concrete Structures. Committee report 352R-85. American Concrete Institute, ACI Journal, 1985; 82(3): 266-284.
[4] ACI Committee 318. Building Code Requirements for Structural Concrete (ACI 318-19) and Commentary (ACI 318R-19). American Concrete Institute. Farmington Hills. MI, 2019. P. 623.
[5] Gençoğlu M, Eren İ. An experimental study on the effect of steel fiber reinforced concrete on the behavior of the exterior beam column joints subjected to reversal cyclic loading. Turk J Eng Environ Sci 2002;26(6):493–502.
[6] Ghobarah A, Aziz TS, Biddah A. Seismic Rehabilitation of Reinforced Concrete Beam-Column Connections. Journal of Earthquake Spectra 1996;12(4):761–80.
[7] Tahnat YBA, Dwaikat MM, Samaaneh MA. Effect of using CFRP wraps on the strength and ductility behaviors of exterior reinforced concrete joint. Compos Struct 2018;2018(201):721–39.
[8] Alkhatib AM. Study of high strength reinforced concrete exterior beam-column joints under cyclic loading. King Fahed Univ Petrul Minirals 2015:1–178.
[9] Hakeem IYA. Characterization of an ultra-high performance concrete. King Fahd University of Petroleum & Minerals (Saudi Arabia); 2011. MSc Thesis.
[10] Graybeal BA. Compressive behavior of ultra-high- performance fiber-reinforced concrete. ACI Mater J 2007;104(2):146–52.
[11] Wuest, J., EPF, C., Brühwiler, E., & ETH, D. Model for predicting the UHPFRC tensile hardening. In Ultra High Performance Concrete (UHPC): Proceedings of the Second International Symposium on Ultra High Performance Concrete, Kassel, Germany, 2008; 10: 153.
[12] Prem PR, Bharatkumar BH, Iyer NR. Mechanical properties of ultra high performance concrete. World Acad Sci, Eng Technol 2012;68:1969–78.
[13] Concretes UHPFR. Documents scientifiques et techniques. Association Française de Génie Civil (AFGC) 2002.
[14] Federal high way administrations. Properties and Behavior of UHPC-Class Materials. Publication FHWA-HRT-18-036, 2018; p. 1-70 and 140-147.
[15] Halahla AM, Rahman MK, Al-Gadhib AH, Al-Osta MA. Baluch, Mohammed H, Experimental investigations and FE simulation of exterior BCJs retrofitted with CFRP fabric. Earthquakes and Structures 2019;17(4):337–54.
[16] Tahnat A, Yazan B, Samaaneh MA, Dwaikat MM, Halahla A. Simple equations for predicting the rotational ductility of fiber-reinforced-polymer strengthened reinforced concrete joints. In: Structures Elsevier 2020:73–86.

[17] Tahnat A, Yazan B, Dwaikat, Mahmud MS, Samaaneh, Mohammad A. Effect of using CFRP wraps on the strength and ductility behaviors of exterior reinforced concrete joint. Comp Struct 2018;201:721–39.
[18] Halahla AM, Tahnat A, Yazan B, Almasri AH, Voyiadjis GZ. The effect of shape memory alloys on the ductility of exterior reinforced concrete beam-column joints using the damage plasticity model. Eng Struct 2019;200:109676.
[19] Abu Tahnat, Yazan B., Halahla, Abdulsamee M., The Effect of Using Ultra High-Performance Concrete at Exterior Reinforced Concrete Joints on the Behavior of an R.C Frame under Seismic Load. International Conference on Earthquake Engineering and Seismology (5ICEES), Ankara, Turkey, 2019.
[20] Shannag MJ, Abu-Dyya N, Abu-Farsakh G. Lateral load response of high performance fiber reinforced concrete beam–column joints. Constr Build Mater 2005;19(7):500–8.
[21] Ganesan N, Indira PV, Sabeena MV. Behaviour of hybrid fibre reinforced concrete beam–column joints under reverse cyclic loads. Mater Des 2014;54:686–93.
[22] Chao SH, Kaka V, Palacios G. Seismic behavior of ultrahigh-performance fiber-reinforced concrete moment frame members. In First international interactive symposium on UHPC–2016. 2016.
[23] Khan MI, Al-Osta MA, Ahmad S, Rahman MK. Seismic behavior of beam-column joints strengthened with ultra-high performance fiber reinforced concrete. Compos Struct 2018;200:103–19.
[24] Al-Osta MA, Isa MN, Baluch MH, Rahman MK. Flexural behavior of reinforced concrete beams strengthened with ultrahigh performance fiber reinforced concrete. Constr Build Mater 2017;134:279–96.
[25] Safdar M, Matsumoto T, Kakuma K. Flexural behavior of reinforced concrete beams repaired with ultra-high performance fiber reinforced concrete (UHPFRC). Compos Struct 2016;157:448–60.
[26] Chen L, Graybeal BA. Modeling structural performance of second-generation ultrahigh-performance concrete pi-girders. J Bridge Eng 2012;17(4):634–43.
[27] Sarmiento PA, Torres B, Ruiz DM, Alvarado YA, Gasch I, Machuca AndrésF. Cyclic behavior of ultra-high performance fiber reinforced concrete beam-column joint. Struct Concr 2019;20(1):348–60.
[28] Hung C-C, Hu F-Y, Yen C-H. Behavior of slender UHPC columns under eccentric loading. Eng Struct 2018;174:701–11.
[29] Racky, P. Cost-effectiveness and sustainability of UHPC. In Proceedings of the International Symposium on Ultra High Performance Concrete, Kassel, Germany, 2004; 797-805.
[30] ABAQUS. ABAQUS Analysis User's Manual Version 6.13. Assault Systems 2013.
[31] Jasim WA, Tahnat A, Yazan B, Halahla AM. Behavior of reinforced concrete deep beam with web openings strengthened with (CFRP) sheet. In: Structures. Elsevier; 2020. p. 785–800.
[32] Halahla A. Identification of crack in reinforced concrete beam subjected to static load using non-linear finite element analysis. Civil Eng J 2019;5(7):1631–46.
[33] Almasri AH, Halahla AM. Effect of tension stiffening on the deflection of a tapered reinforced concrete cantilever under a concentrated load. Internat Rev Civil Eng 2019;10(2):56–62.
[34] Almassri B, Halahla AM. Corroded RC beam repaired in flexure using NSM CFRP rod and an external steel plate. In: Structures. Elsevier; 2020. p. 343–51.
[35] Saenz LP. discussion of" Equation for the Stress-Strain Curve of Concrete" by Desayi and Krishnan. J Am Concr Inst 1964;61:1229–35.
[36] Nayal R, Rasheed HA. Tension stiffening model for concrete beams reinforced with steel and FRP bars. J Mater Civ Eng 2006;18(6):831–41.
[37] Hu MS, Evans AG. The cracking and decohesion of thin films on ductile substrates. Acta Metall 1989;37(3):917–25.
[38] Luccioni B, Oller S, Danesi R. Coupled plastic-damaged model. Comput Methods Appl Mech Eng 1996;129(1-2):81–9.
[39] Burlion N, Gatuingt F, Pijaudier-Cabot G, Daudeville L. Compaction and tensile damage in concrete: constitutive modelling and application to dynamics. Comput Methods Appl Mech Eng 2000;183(3-4):291–308.
[40] Birtel V, Mark P. Parameterised finite element modelling of RC beam shear failure. In: ABAQUS users' conference; 2006. p. 95–108.
[41] Nasrin S, Ibrahim A, Al-Osta M, Khan U. Behavior of retrofitted UHPC beams using carbon fiber composites under impact loads. In: Structures Congress 2017; 2017. p. 392–402.
[42] Al-Osta MA, Khan U, Baluch MH, Rahman MK. Effects of Variation of axial load on seismic performance of shear deficient RC exterior BCJs. Internat J Concr Struct Mater 2018;12(1):46.
[43] Ashour MJ, Elmezaini N. Nonlinear analysis of concrete beams strengthened with steel fiber-reinforced concrete layer. Nonlinear Anal Concr Beams Strength Steel Fiber-Reinforced Concr Layer 2015;2(3):181–8.
[44] Park R, Paulay T, editors. Reinforced concrete structures. Wiley; 1975.
[45] Cohn MZ, Bartlett M. Computer-simulated flexural tests of partially pre-stressed concrete sections. ASCE J Struct Div 1982;108(12):2747–65.
[46] Azizinamini A, Pavel R, Hatfield E, Gosh SK. Behavior of lap spliced reinforcing bars embedded in high strength concrete. ACI Struct J 1999:826–36. https://doi.org/10.14359/737.
[47] Bernardo LFA, Lopes SMR. Neutral axis depth versus flexural ductility in high-strength concrete beams. J Struct Eng 2004;130(3):452–9.